Submitted to ADVANCED MATERIALS

DOI: 10.1002/adma.((please add manuscript number))

Addressable and Color-Tunable Piezophotonic Light-emitting Stripes

By *Yan Chen, Yang Zhang*, Daniil Karnaushenko, Li Chen, Jianhua Hao, Fei Ding, and Oliver G. Schmidt*

Y. Chen, Dr. Y. Zhang, D. Karnaushenko, Dr. F. Ding, Prof. O. G. Schmidt
Institute for Integrative Nanosciences
IFW Dresden
Helmholtzstraße 20, 01069 Dresden, Germany
E-mail: yang.zhang@ifw-dresden.de
Prof. O. G. Schmidt
Material Systems for Nanoelectronics
Technische Universität Chemnitz
09107 Chemnitz, Germany

L. Chen, Prof. J. Hao
Department of Applied Physics
The Hong Kong Polytechnic University
Hong Kong, China
The Hong Kong Polytechnic University Shenzhen Research Institute
Shenzhen 518057, P. R. China

Keywords: (piezophotonic luminescence, color-tunable, addressable, PMN-PT, thin film)

As an emerging solid-state lighting (SSL) technology, piezophotonic light-emitting devices have great potential for future micro- and nanoscale systems due to the added functionality provided by the electromechanical transduction coupled with the ability of light emission.[1] The piezophotonic effect is a two-way coupling effect between piezoelectricity and photoexcitation properties, where the strain-induced piezoelectric potential modulates the band structure within piezoelectric phosphors, and thus tunes/controls the relevant optical process.[2, 3] The realization of light emission stimulated by the piezophotonic effect is to initiate the mechanoluminescence (ML) process replacing p-n junction based light-emitting diodes (LEDs) for general lighting purposes. ML emission triggered by mechanical sources offers an enticing range of possibilities, for example, dual-mode ultrasound probes,[4] wind-driven displays,[5] acoustically induced piezo-luminescence,[6] etc. Very recently, a dynamic

pressure-distribution mapping device based on the ML process was realized, which promised prospective applications in real-time pressure sensing, security systems and human-machine interfaces.[2] The most common and controllable piezophotonic luminescence devices are composed of ML phosphor coated on the top of piezoelectric actuators. Relaxor ferroelectric single-crystal $Pb(Mg_{1/3}Nb_{2/3})O_3$-$PbTiO_3$ (PMN-PT) has superior piezoelectric coefficients (d_{33} > 1500 pm/V) and electromechanical coupling factors (k_{33} > 90%) along the [001] crystallographic direction, which has been widely used as active actuators. PMN-PT could generate large linear forces under applied voltages with fast actuation.[7] Piezophotonic luminescence devices incorporating PMN-PT have been used for electrical-controllable light emission.[4] Up to now, all the PMN-PT actuators used for piezophotonic luminescence purposes are made from single-crystal bulk materials ranging from 0.5 to 1 mm thickness. Piezophotonic light-emitting sources based on PMN-PT bulk are severely restricted by many challenges, such as a high voltage burden (up to hundreds of volts), low integration density and micro-manufacturing difficulties. Also, it is difficult to integrate many piezoelectric elements with different patterns together on a single chip. To fabricate a large-area array with each element being addressable would promise dramatically greater design freedom for the realization of smaller light-emitting elements, facilitating its applications as light sources and displays. Developing chip-integrated devices or incorporating such photonic components onto a Si platform is even more highly sought after in this field.

Utilizing piezoelectric thin films as central active elements is an appealing alternative way to overcome all these problems.[8] One approach to obtain PMN-PT thin films is to directly grow the PMN-PT on the Si substrate. There has been a lot of effort towards the growth of PMN-PT thin films on silicon substrates.[9] However, the piezoelectric quality is still not comparable to single-crystal PMN-PT films. In this work, a patterned single-crystal PMN-PT thin film of 7 μm thickness is obtained as the active layer. Zinc sulfides doped with Mn, Cu and Al ions (ZnS:Mn and ZnS:Cu,Al) were selected as the phosphors due to their intense and durable ML

characteristics.[10, 11] The utilization of piezoelectric thin films strongly reduces the voltage burden, and allows us to take advantage of mature micro-manufacturing techniques. An array of actuators has been produced from the single-crystal PMN-PT thin film, with each active element having a footprint of 120 μm in length and 100 μm in width. Each actuator can be individually addressed generating local deformation to trigger piezoluminescence. Color tunability by controlling the bias voltage can provide an extra degree of freedom for light-emitting devices with new potential applications. A stacked device structure composed of two or more ML layers with different spectral energy distributions can realize continuous and reversible tuning of the piezophotonic luminescence. Here, the color from a bilayer of ZnS:Cu,Al and ZnS:Mn has been tuned in an in-situ and real-time manner, by merely regulating the strain rate. Our device opens up a new prospective way to develop Si-integrated addressable and color-tunable piezophotonic light-emitting components.

Figure 1a schematically illustrates the device fabrication process. The (001)-oriented single-crystal PMN-PT was bonded on Si. Then it was mechanically grinded down to tens of microns. However, to pattern PMN-PT films with such thickness still remains challenging. To further thin down the films, instead of mechanical grinding, we turn to inductively coupled plasma reactive ion etching (ICP-RIE). Compared with other etching methods such as wet chemical etching, the ICP-RIE can produce a very smooth surface. The etching rate and surface roughness can be well controlled by adjusting the etching process, including etching gases, substrate bias, RF power and chamber temperature, etc. In this work, we choose the combination of SF_6 and Ar as the etching gases. The RF power was set to generate a moderate plasma to obtain a smooth surface. We etched the PMN-PT film down to 7 μm thickness, thin enough for further pattern. Afterwards photolithography and gold sputtering were used to define the array of top contacts. We used focused ion beam (FIB) to etch the trenches into the single crystal PMN-PT thin film around the top contacts. **Figure 1b** shows the scanning electron microscopy (SEM) image of an array of the etched PMN-PT actuators on Si. Each

element has a footprint of 120 μm × 100 μm. The inset of Figure 1b shows the details of the trenches in the film. The trenches are deep enough to penetrate into the silicon substrate, facilitating subsequent undercut etching. The wet chemical undercut etching was used to release the single-crystal PMN-PT thin film from the substrate. As shown in SEM image, no cracks on the PMN-PT were found after the processing. The distinctive cantilever geometry of the single-crystal PMN-PT thin film is likely to be important to reduce the clamping strain and improve the piezoelectric response.[12] Further structural and compositional characterization of the etched PMN-PT thin film was performed by X-ray diffraction (XRD). As shown in **Figure 1c**, X-ray θ-2θ scans display only (00*l*) diffraction peaks of a pure perovskite phase of PMN-PT, confirming the micro-processing does not introduce any secondary phase or impurities into the thin film. This is essential to guarantee that the PMN-PT thin film preserves the giant piezoelectric properties comparable to its bulk counterpart. The polarization properties of the as-prepared suspended PMN-PT thin film were studied by measuring the hysteresis loop (*P*-*V* curve) over a voltage range from -20 to 20 volts. As shown in **Figure 1d**, the hysteresis loop recorded at 1 kHz was found to be symmetric and saturated. The remanent polarization (P_r) is determined to be 25.9 μC/cm^2, which is comparable to the reported value of single-crystal PMN-PT film.[13] The measured hysteresis loop confirms the preservation of ferroelectricity of the suspended PMN-PT thin film. **Figure 1e** shows the calculated piezoelectric displacement of the PMN-PT cantilever under a direct current (DC) voltage using a COMSOL software. The simulation shows the enhanced piezoelectric response of the free-standing PMN-PT, as well as the strain distribution. We also measured the impedance and phase spectra of the free-standing PMN-PT actuator as a function of frequency as shown in **Figure 1f**. The resonance frequency is found at approximately 106 MHz, which is one order of magnitude higher than the previously reported value for PMN-PT bulk and this suggests that the cantilever can be used to develop high frequency ultrasound transducers, mass detectors and many other applications.

ZnS:Mn thin films were afterwards deposited onto the PMN-PT actuators. To investigate the crystalline phases of the ZnS:Mn films, the XRD patterns of the ZnS:Mn films on the PMN-PT thin film are shown in **Figure 2a**. The XRD diffraction peaks can be well indexed to wurtzite phase ZnS (JCPDS No. 36-1450). Except for the peaks of the PMN-PT and Au layers, no additional peaks associated with a secondary phase or impurities were found, revealing the high purity of the as-synthesized ZnS:Mn films. Only (002) and (004) diffraction peaks of wurtzite-type ZnS:Mn were observed, indicating the *c*-axis preferred orientation of the films. The cross-section SEM image (**Figure 2b)** shows the ZnS:Mn layer has a smooth surface and uniform thickness of 500 nm.

The backside of the single-crystal PMN-PT thin film is wired out as the bottom contact. When an alternating current (AC) peak-to-peak voltage (V_{pp}) of 20 V at 150 Hz is applied to the PMN-PT in vertical direction, a normalized ML spectrum of the ZnS:Mn thin film is shown in **Figure 3a**. For comparison, photoluminescence (PL) of the ZnS:Mn film under 447 nm laser excitation is also presented in Figure 3a. The dominant peak is found at approximately 592 nm in the ML spectrum, which is similar to the observation in the PL spectrum. This indicates that the electric-field induced piezoluminescence also results from the $^4T_1 \rightarrow {}^6A_1$ transition of the Mn^{2+} ion. The wurtzite-type Mn^{2+}-doped ZnS possesses a non-central symmetric structure and inherently exhibits piezoelectric characteristics.[14] The in-plane strain of the ZnS:Mn film can be reversibly and nearly linearly controlled by the voltage applied vertically across the PMN-PT thin film. The imposed strain lifts the piezoelectric potential, which tilts the conduction and valence bands of ZnS as shown in **Figure 3b**. A first principle calculation confirms Mn^{2+} ion doping introducing electron and hole defect states between the conduction and valence bands. The electron in the upper electron defect state detraps and escapes into the conduction band. Then the detrapped electrons recombine with the holes non-radiatively, and transfer the energy to the Mn^{2+} ions. When the Mn^{2+} ion returns from the excited state ($^4T_1$) to the ground state ($^6A_1$), a photon is emitted.[2] From Figure 3b, we can find that that magnitude

of strain determines the tilt angle of the conduction band, which decides the amount of detrapped electrons. Hence, a larger strain results in more intense piezoluminescence, which is confirmed by the following experiment. **Figure 3c** shows the transient luminescence of the device when applying a square voltage to the PMN-PT. It is interesting to find that pulsed emission of luminescence only appears when the bias is switched on and off. If the bias keeps unchanged, the piezoluminescence fades away. The attenuation of the piezoluminescence can be ascribed to the depletion of detrapped electrons. Under a fixed strain, only a certain number of detrapped electrons escape into the conduction band. Hence, the piezoluminescence will extinguish with the detrapped electrons exhausting. Once the strain is released, the tilt conduction band becomes flat. The electrons will redistribute, while the traps will be refilled. So only a constantly oscillating strain can sustain the piezoluminescence. If applying a direct current (DC) voltage on PMN-PT film, no luminescence can be detected. So the strain-induced piezoluminescence should be a dynamic process. When the maximum value is reached, the luminescence intensity decreases exponentially with time. We note that the decay time of the luminescence at the rising edges is much faster than that at the falling edges. Similar results were previously observed in the transient luminescence from oriented ZnS:Mn films on PMN-PT bulks.[3] When applying a positive or negative bias to the PMN-PT, the lattice of the PMN-PT thin film will change in an opposite manner, i.e., expanding or contracting along the *c* axis, respectively. As a consequence of the Poisson effect, we speculate the in-plane strain-induced potential has different polarities, which may result in the different profiles of transient luminescence at the bias switching edges. This observation differs from the studies of ZnS:Cu,Al + PDMS composites[15] where the transient luminescence of ZnS:Cu,Al + PDMS composites was found to exhibit a similar response to the rising and falling edges, which was ascribed to the random crystal orientation of polycrystalline ZnS:Cu,Al powder. These results confirm our hypothesis.

Figure 4 shows the piezoluminescence intensity as a function of the frequency and magnitude of the applied voltage. The luminescence intensity (I) of ML is proportional to the strain (σ) and its change rate ($\partial\sigma/\partial t$), which can be written in the form:[16]

$$I = \alpha\sigma\frac{\partial\sigma}{\partial t}\left(1-\exp\left(-\frac{t}{\tau}\right)\right) \quad (1)$$

where α is a constant describing the strain coupling to ML; τ is the lifetime of the interaction associated with the ML. The strain (σ) created by the converse piezoelectric effect is expressed as

$$\lambda = \frac{\partial\sigma}{\partial E} = d\frac{\partial\sigma}{\partial V} \quad (2)$$

where λ is piezoelectric coefficient. E and V are the electric field and voltage, respectively; d is the thickness of the piezoelectric film. Equation (1) can be expressed as

$$I = \alpha\lambda\frac{\sigma}{d}\frac{\partial V}{\partial t}(1-\exp(-\frac{t}{\tau})) \quad (3)$$

According to Equation (3), it is known that a static DC electric field is unable to excite ML due to $\partial V/\partial t = 0$. A periodic electric signal is applied to the single-crystal PMN-PT thin film. We average the luminescence intensity I during one time period. The averaged ML intensity (I_a) can be written as[17]

$$I_a = \frac{1}{T}\int_0^T I dt = f*\int_0^T \alpha\lambda\frac{\sigma}{d}\frac{\partial V}{\partial t}(1-\exp(-\frac{t}{\tau}))dt \quad (4)$$

T and f are the time period and frequency of external electric voltage applied to the single-crystal PMN-PT thin film, respectively. For $t \gg \tau$, I_a can be expressed as

$$I_a = f*\int_0^{V_0}\alpha\lambda\frac{\sigma}{d}dV = \frac{1}{2}f\alpha\lambda^2\left(\frac{V_0}{d}\right)^2 \quad (5)$$

where V_0 is the maximum value of the voltage applied on PMN-PT thin film. From equation (5), we can see that the total ML intensity has a positive linear relationship with f and V_0^2. And experimentally the luminescence intensity increases linearly when increasing the frequency from 25 to 150 Hz as shown in **Figure 4a** and **b**. The luminescence intensity is also enhanced

by an increase of the applied voltage from 8 to 24 V_{pp} (**Figure 4c**). Note that the ML intensity almost increases linearly with increasing V_0^2, which is consistent with the proposed model (**Figure 4d**). Photographs of tunable light emissions from the ZnS:Mn stripe is demonstrated in **Figure 4e**. The piezophotonic device reaches a luminous efficacy of 1.2 lm/W at 24 V_{pp} and 150 Hz. The brightness increased linearly with the increasing frequency as shown in Figure 4e. The luminance values were found to be 20.8 cd/m^2, 41.5 cd/m^2, and 64.2 cd/m^2, at the frequencies of 50 Hz, 100 Hz, and 150 Hz, respectively, while the applied voltage kept at 24 V_{pp}.

The ability to individually control the chip-integrated piezophotonic components is highly desirable. Incorporating such components onto a Si platform should be appealing for developing on-chip piezophotonic devices. The integration of such devices on PMN-PT bulk has been challenging because of the large footprint of individual light-emitting elements, high voltage burden, and high production costs. Here, we demonstrate a prototype piezophotonic device to circumvent these challenges. **Figure 5a** shows the sketch of such a device. Four light-emitting units are encoded from A to D, which can be electrically triggered independently. Each unit can produce local deformation not influenced by others. **Figure 5b** demonstrates the addressable characteristics of the device. When all the external voltage is switched off, there is no light-emission observed from all the four units (situation i). To individually address each unit, we first trigger unit A with 24 V_{pp} at 150 Hz and bright light can be observed in unit A only (situation ii). In situation iii, we switch off unit A, and excite units B and C. As shown in Figure 5b, only units B and C glow. Situation iv shows that four elements are triggered simultaneously. The addressability shown here promises more flexibility for many intriguing applications, especially when used as light sources or displays with each unit as active pixel.

The ability to manipulate the color of the piezophotonic luminescence is highly desirable. By regulating the mixing ratio of two or more ML materials can realize color tuning. However, it

is essentially an irreversible and ex-situ method. Previous research reported that the ML spectrum of ZnS:Cu,Al shifted to short wavelength as the strain rate was increased,[18] due to the increasing recombination of the electrons in the conduction band (or shallow donor level) and holes in the valence band (or the *e* state of Cu).[19] The normal mechanical stretching-releasing system can only provide the strain rate up to several hundred Hertz.[10] Thus shifts of only several nanometers were observed. Here, our electrical-triggered PMN-PT based device can be stimulated up to megahertz, which is suitable for realizing color manipulation of ML from ZnS:Cu,Al contained phosphor layers. **Figure 6a** shows the spectral shape of ZnS:Cu,Al under the frequencies increased from 50 Hz to 100 kHz, the applied voltage was kept at 20 V_{pp}. The spectra are normalized to the peak of ZnS:Cu,Al at 522 nm for intuitively showing the changes. With the strain rate increased, the light emission of ZnS:Cu,Al around 460 nm enhances and gradually dominates the emission. The calculated Commission Internationale de L'Eclairage (CIE) coordinates clearly suggest the shift from (0.27, 0.57) at 50 Hz to (0.20, 0.30) at 100 kHz (**Figure 6c**). In order to obtain a more colorful patterned device, a bilayer film composed of ZnS:Cu,Al and ZnS:Mn was deposited on the PMN-PT. **Figure 6b** shows the normalized spectra of ZnS:Cu,Al/ZnS:Mn bilayer. The calculated spectra is normalized by the peak wavelength of the ZnS:Mn. Results have shown that the spectral shape of ZnS:Mn is unchanged with increasing frequency, which is consistent with previous reports.[10] While, the intensity of ZnS:Cu,Al clearly increases. The calculated CIE coordinates shift from (0.39, 0.50) to (0.26, 0.31) with the frequency increasing from 50 Hz to 100 kHz for the ZnS:Cu,Al/ZnS:Mn bilayer emission. As a result, a color-tunable light emission from orange to blue-green is obtained. These results imply that continuous and reversible controllable color manipulation can be achieved through real-time regulating the strain actuating rate.

In summary, we have demonstrated chip-integrated, addressable and color-tunable piezophotonic light-emitting devices based on the metal ions doped-ZnS/PMN-PT heterostructure. The piezophotonic luminescence is induced by the piezoelectric potential via

strain-mediated coupling, and the light emission can be modulated in reversible and dynamic manner via control of the magnitude and frequency of the operation voltage applied to the single-crystal PMN-PT thin films. In comparison to its bulk counterparts, the devices incorporating single-crystal PMN-PT thin films have several improved figures of merit. First, the utilization of PMN-PT thin film strongly reduces the voltage burden for the devices. Suspended PMN-PT thin films generate the required strain under reduced voltages of only 10 to 20 volts. Second, thin film structures benefit from efficient micro-manufacturing processes, which promises great design freedom for on-chip integration. The realization of addressable light-emitting units with small footprint enables scalable on-chip light sources. And finally, continuous and reversible controllable color manipulation has been demonstrated through real-time regulating the strain actuating rate of the PMN-PT film. Our proof-of-concept device solves the main problems hampering the applications of piezophotonic luminescence devices (e.g., high voltage burden, not addressable, and low integration density, etc.) and offers the possibility to develop more compact and colorful piezophotonic light sources and displays.

Experimental

Device Fabrication: Cr/Au (30 nm/100 nm) bi-layer coated (001)-oriented PMN-PT single-crystal was bonded on silicon wafer by adhesive epoxy. Then the PMN-PT crystal was thinned down to a thickness of 7 um using grinding, subsequent mechanical polishing and ICP-RIE. Cr/Au (5 nm/100 nm) layer was thermally evaporated on the surface of PMN-PT as top electrode, as well as a stiff strain-transfer layer. Focused ion beam (FIB) was used to etch PMN-PT and metal layers to define the actuator structure. Wet chemical etching was used to release the PMN-PT thin films from the substrate. ZnS:Mn (500 nm) and ZnS:Cu,Al/ZnS:Mn (250 nm/250 nm) thin films were afterwards grown on the PMN-PT by pulsed laser deposition (PLD) with a KrF excimer laser (wavelength 248 nm). The laser pulse repetition

frequency and energy density were 5 Hz and 2 J cm^{-2}, respectively. The substrate temperature and base pressure of the vacuum chamber were fixed at 200 °C and 1×10^{-6} mbar. After deposition, the films were slowly cooled down to room temperature.

Characterization and Luminescence Measurement: The XRD measurement was carried out using the Bruker D8 Advance x-ray diffractometer. SEM and FIB were performed on a Zeiss NVision 40 FIB-SEM. The Polarization hysteresis loops were measured with a Radiant Multiferroic testing system. PMN-PT film was polarized by a Keithley 2410 source meter. The AC signals applied on the sample were produced using a Tektronix AFG3101 Arbitrary/Function generator connected with a voltage amplifier. The dielectric properties were carried out on a precision impedance analyzer 4294A (Agilent, USA). The luminescence measurements were recorded using a micro-PL/Raman system (InVia, Renishaw) with a 447 nm laser as excitation source. The transient luminescence was measured with high-speed photodetector (DET10A/M Si Detector). A spectroradiometer (PR-670, Photo Research Inc.) was used to measure the luminance. The light-emitting images were captured by an inverted optical microscope (IX-71, Olympus). All measurements were carried out at room temperature.

Acknowledgements

The work was supported by Alexander von Humboldt Foundation, German Research Foundation (DFG) under project DI 2013/2-1, and German Federal Ministry of Education and Research (BMBF) under project Q.Com-H (16KIS0106). J.H. acknowledges National Natural Science Foundation of China (No. 11474241).

Received: ((will be filled in by the editorial staff))
Revised: ((will be filled in by the editorial staff))
Published online: ((will be filled in by the editorial staff))

[1] L.-B. Huang, G. Bai, M.-C. Wong, Z. Yang, W. Xu, J. Hao, Advanced Materials 2016, 28, 2744; S. M. Jeong, S. Song, H. Kim, Nano Energy 2016, 21, 154; F. Xue, L. Chen, J. Chen, J. Liu, L. Wang, M. Chen, Y. Pang, X. Yang, G. Gao, J. Zhai, Z. L. Wang, Advanced Materials 2016, 28, 3391.
[2] X. Wang, H. Zhang, R. Yu, L. Dong, D. Peng, A. Zhang, Y. Zhang, H. Liu, C. Pan, Z. L. Wang, Advanced Materials 2015, 27, 2324.
[3] C. Pan, M. Chen, R. Yu, Q. Yang, Y. Hu, Y. Zhang, Z. L. Wang, Advanced Materials 2016, 28, 1535.
[4] Y. Zhang, G. Gao, H. L. W. Chan, J. Dai, Y. Wang, J. Hao, Advanced Materials 2012, 24, 1729.
[5] S. M. Jeong, S. Song, K.-I. Joo, J. Kim, S.-H. Hwang, J. Jeong, H. Kim, Energy & Environmental Science 2014, 7, 3338.
[6] M. Kersemans, P. F. Smet, N. Lammens, J. Degrieck, W. Van Paepegem, Applied Physics Letters 2015, 107, 234102.
[7] C.-B. Eom, S. Trolier-McKinstry, MRS Bulletin 2012, 37, 1007; Y. Chen, I. E. Zadeh, K. D. Jöns, A. Fognini, M. E. Reimer, J. Zhang, D. Dalacu, P. J. Poole, F. Ding, V. Zwiller, O. G. Schmidt, Applied Physics Letters 2016, 108, 182103.
[8] S.-H. Baek, M. S. Rzchowski, V. A. Aksyuk, MRS Bulletin 2012, 37, 1022; Y. Chen, J. Zhang, M. Zopf, K. Jung, Y. Zhang, R. Keil, F. Ding, O. G. Schmidt, Nat Commun 2016, 7.
[9] S. H. Baek, J. Park, D. M. Kim, V. A. Aksyuk, R. R. Das, S. D. Bu, D. A. Felker, J. Lettieri, V. Vaithyanathan, S. S. N. Bharadwaja, N. Bassiri-Gharb, Y. B. Chen, H. P. Sun, C. M. Folkman, H. W. Jang, D. J. Kreft, S. K. Streiffer, R. Ramesh, X. Q. Pan, S. Trolier-McKinstry, D. G. Schlom, M. S. Rzchowski, R. H. Blick, C. B. Eom, Science 2011, 334, 958; M. Detalle, G. Wang, D. Rémiens, P. Ruterana, P. Roussel, B. Dkhil, Journal of Crystal Growth 2007, 305, 137; Y. Tang, D. Zhou, F. Wang, D. Sun, W. Shi, H. Luo, G. Hu, Journal of Alloys and Compounds 2012, 529, 44.
[10] S. M. Jeong, S. Song, S.-K. Lee, N. Y. Ha, Advanced Materials 2013, 25, 6194.
[11] N. Terasaki, H. Zhang, H. Yamada, C.-N. Xu, Chemical Communications 2011, 47, 8034; V. K. Chandra, B. P. Chandra, P. Jha, Applied Physics Letters 2013, 103, 161113.
[12] R. N. Torah, S. P. Beeby, N. M. White, Journal of Physics D: Applied Physics 2004, 37, 1074.
[13] G.-T. Hwang, H. Park, J.-H. Lee, S. Oh, K.-I. Park, M. Byun, H. Park, G. Ahn, C. K. Jeong, K. No, H. Kwon, S.-G. Lee, B. Joung, K. J. Lee, Advanced Materials 2014, 26, 4880.
[14] Z. L. Wang, Nano Today 2010, 2010, 540.
[15] L. Chen, M.-C. Wong, G. Bai, W. Jie, J. Hao, Nano Energy 2015, 14, 372.
[16] R. Sharma, D. P. BiSen, B. P. Chandra, Journal of Electronic Materials 2015, 44, 3312; B. P. Chandra, C. N. Xu, H. Yamada, X. G. Zheng, Journal of Luminescence 2010, 130, 442.
[17] M.-C. Wong, L. Chen, M.-K. Tsang, Y. Zhang, J. Hao, Advanced Materials 2015, 27, 4488.
[18] S. W. Shin, J. P. Oh, C. W. Hong, E. M. Kim, J. J. Woo, G.-S. Heo, J. H. Kim, ACS Applied Materials & Interfaces 2016, 8, 1098.
[19] S. Moon Jeong, S. Song, S.-K. Lee, B. Choi, Applied Physics Letters 2013, 102, 051110.

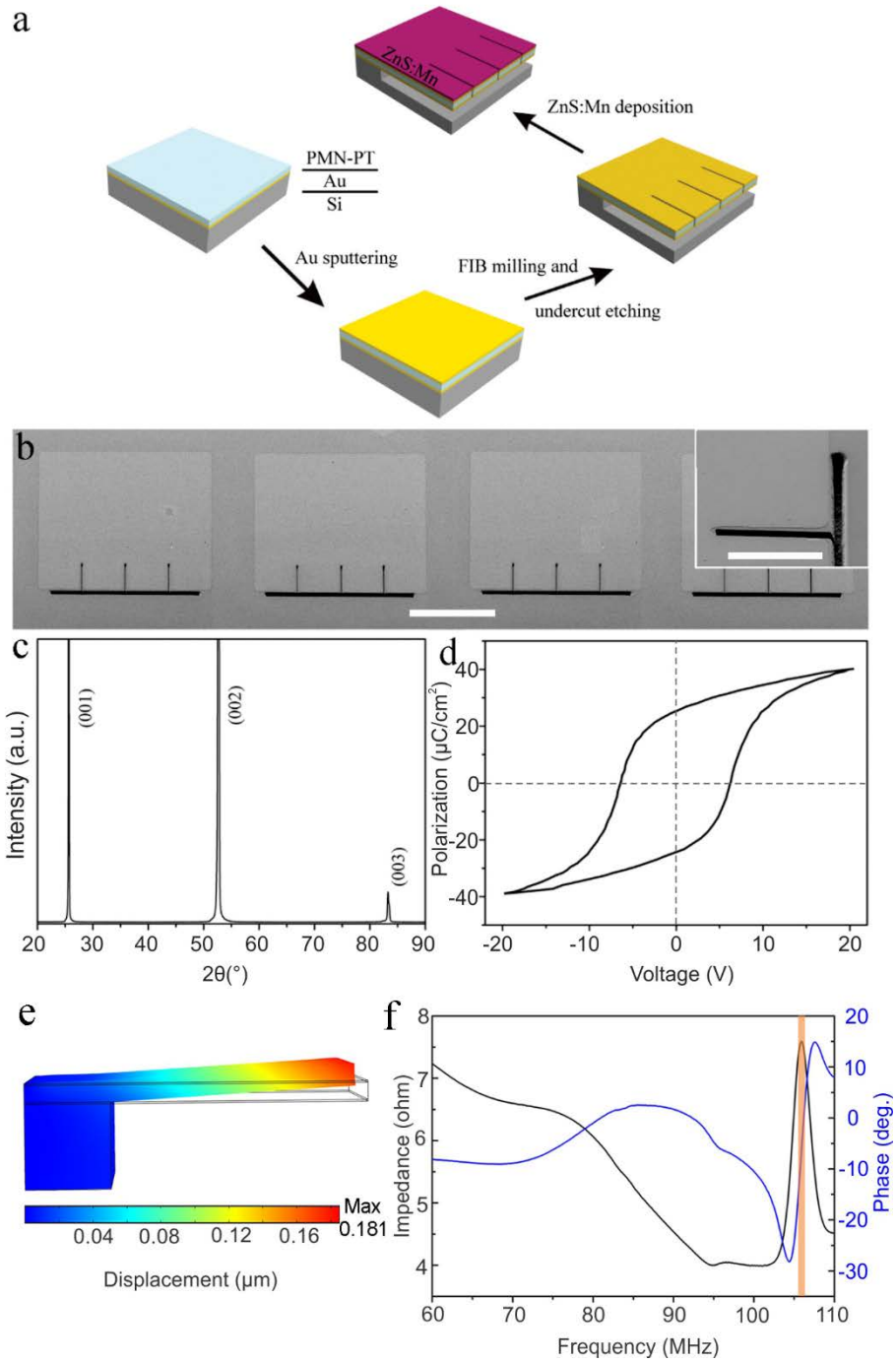

Figure 1. a) Schematic illustration of the device fabrication process. b) SEM image of an array of patterned single-crystal PMN-PT actuators. Scale bar, 50 μm. The inset shows the details of the trenches in the PMN-PT thin film. Scale bar, 20 μm. c) XRD pattern of the etched single-crystal PMN-PT thin film. d) Polarization-voltage (*P*-*V*) hysteresis loop of the etched single-crystal PMN-PT thin film. e). Simulated result of piezoelectric deformation of free-standing PMN-PT cantilever under DC bias. f) Electrical impedance and phase spectra of

the free-standing single-crystal PMN-PT thin film. Orange shadow indicates the resonant frequency of 106 MHz.

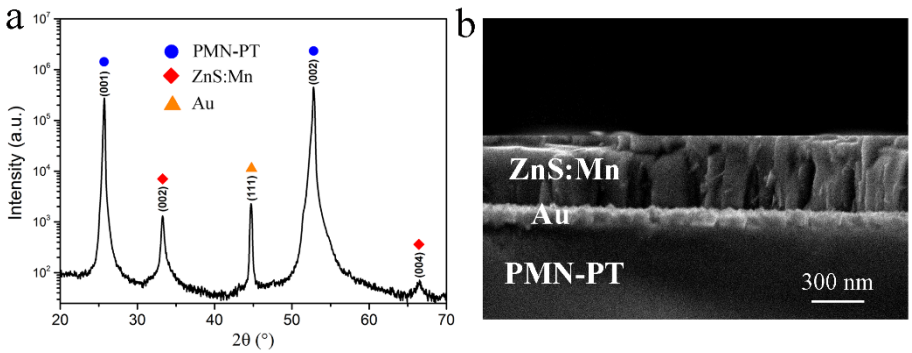

Figure 2. a) XRD pattern of the ZnS:Mn/PMN-PT heterostructure, confirming the *c*-axial oriented wurtzite-type ZnS:Mn film. b) Cross-section SEM image of the ZnS:Mn thin film on an Au-coated single-crystal PMN-PT thin film.

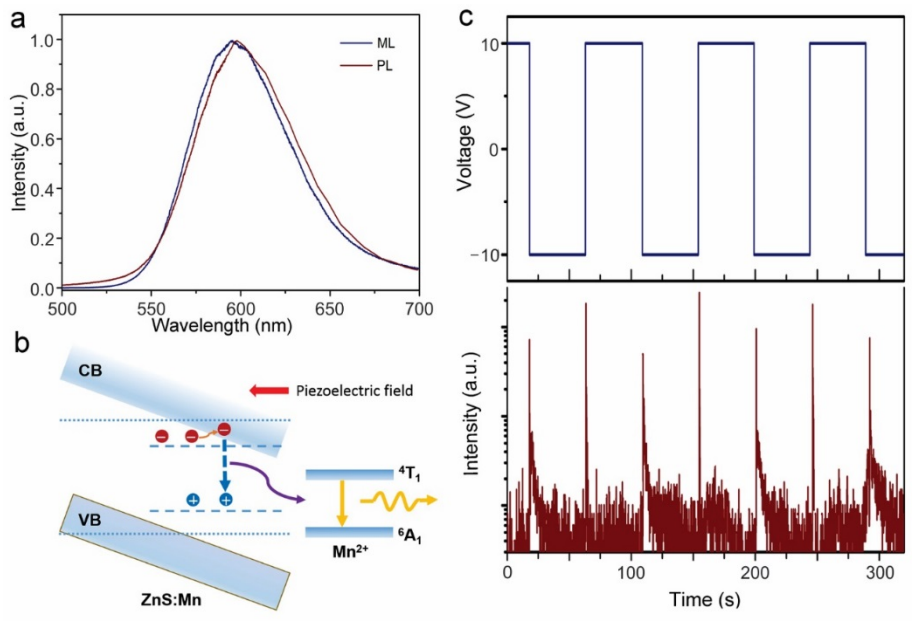

Figure 3. a) Piezophotonic luminescence spectrum of the ZnS:Mn/PMN-PT structure operating at 20 V_{pp} and 150 Hz. PL spectrum of ZnS:Mn excited by 447 nm laser line is also given for comparison. b) Mechanism of the piezophotonic effect initiating the ML process. c)

Transient luminescent property of the device. Square voltage applied to PMN-PT thin film (top), and luminescence intensity at 596 nm as a function of time (bottom).

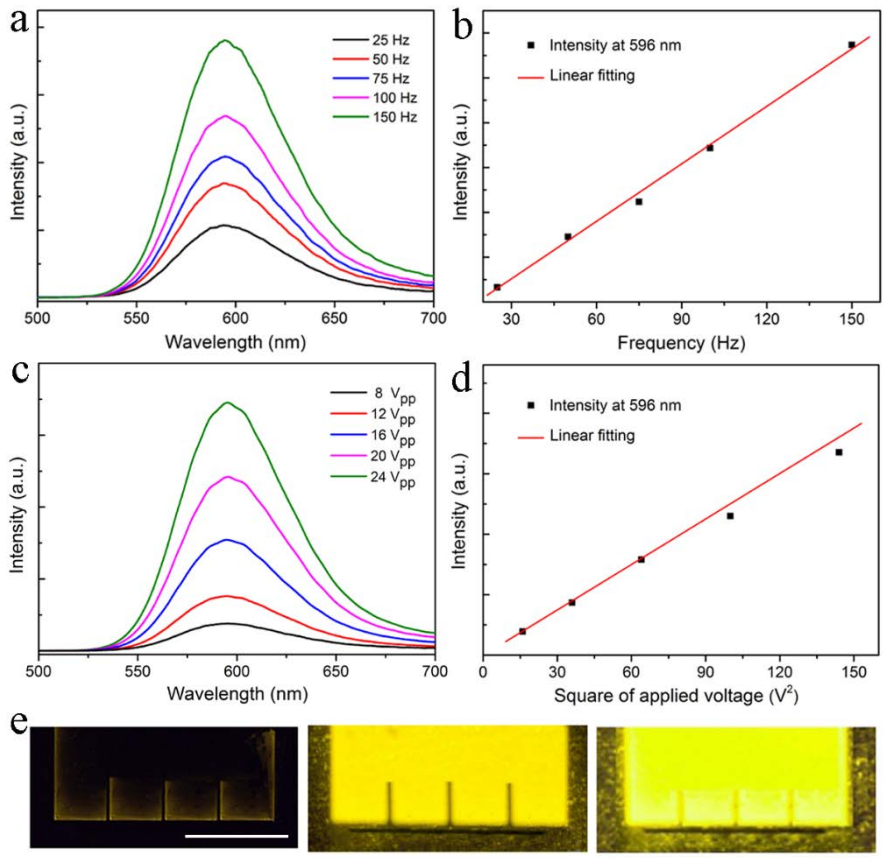

Figure 4. Piezophotonic luminescence under varying frequency and amplitude of the applied voltage. a) Luminescence spectra at different frequencies under fixed voltage 20 V_{pp}. b) Peak intensity at 596 nm versus applied frequency. c) Luminescence spectra under different voltage amplitudes at 150 Hz. d) Peak intensity at 596 nm versus square of amplitude. e) Light-emitting images of ZnS:Mn stripes operating with 24 V_{pp}, and at varying frequencies of 50, 100, and 150 Hz (left to right, respectively). Scale bar indicates 50 μm.

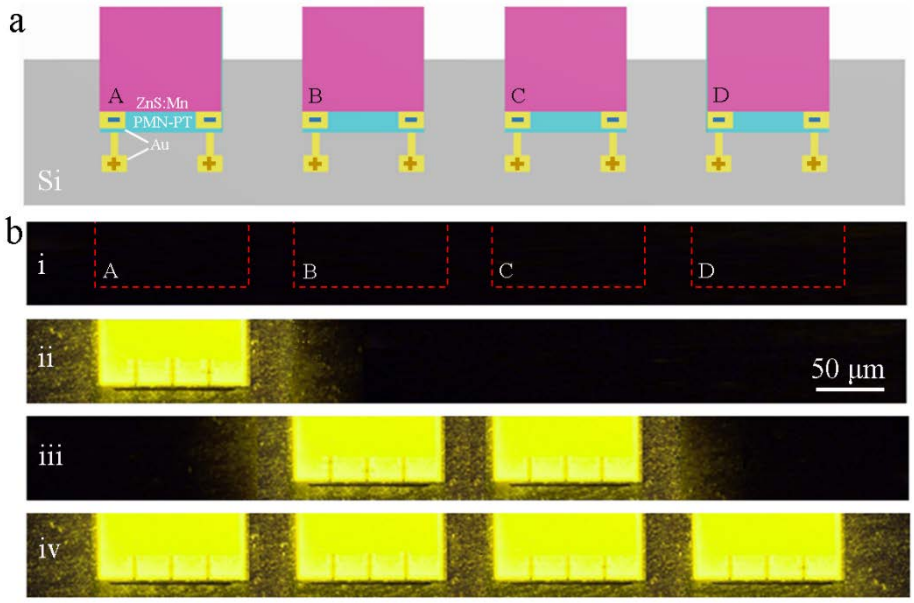

Figure 5. Visualization of addressable piezophotonic light-emitting devices. a) Schematic illustration of the prototype device. Four individual light-emitting units are addressed: A, B, C, and D, from left to right, respectively. Each unit incorporates ZnS:Mn layer (purple), PMN-PT thin film actuator (blue), and top and bottom Au electrodes (yellow). The whole device is integrated on Si (gray). b) Demonstration of four representative addressable light emission states. Switch-off of all units (i); Trigger unit A solely (ii); Turn on units B and C simultaneously (iii); Turn on all units (iv).

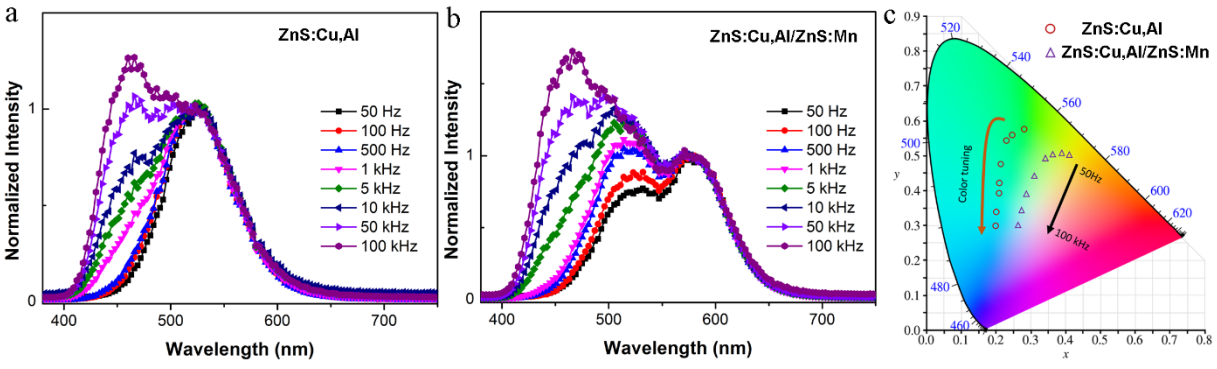

Figure 6. The normalized piezophotonic luminescence spectra under the selective frequency conditions a) ZnS:Cu,Al film and b) ZnS:Cu,Al/ZnS:Mn bilayer film. c) The CIE coordinates showing the color tuning with the frequency increasing.

The table of contents entry should be fifty to sixty words long, written in the present tense, and refer to the chosen figure.

An independently controlled, color-tunable piezophotonic light-emitting device is constructed with a vertically stacked layer architecture that allows addressable tuning of emission color and intensity. The proof-of-concept device solves the main problems hampering the applications of piezophotonic luminescence devices, such as high voltage burden, not addressable, and low integration density, etc. This novel device offers a prospective way to develop Si-integrated addressable and color-tunable piezophotonic light-emitting components.

Keyword (piezophotonic luminescence, color-tunable, addressable, PMN-PT, thin film)

Yan Chen, Yang Zhang, Daniil Karnaushenko, Li Chen, Jianhua Hao, Fei Ding, and Oliver G. Schmidt*

Addressable and Color-Tunable Piezophotonic Light-emitting Stripes

ToC figure ((55 mm broad, 50 mm high, or 110 mm broad, 20 mm high))

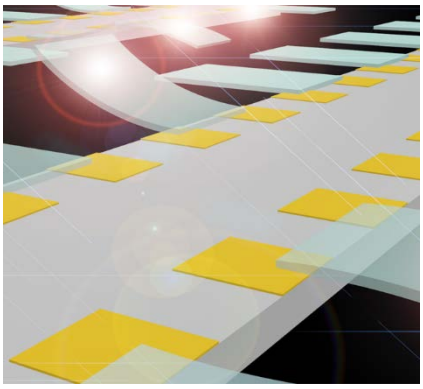

Supporting Information should be included here (for submission only; for publication, please provide Supporting Information as a separate PDF file).